

Article

Functionality Loss and Recovery Time Models for Structural Elements, Non-Structural Components, and Delay Times to Estimate the Seismic Resilience of Mexican School Buildings

Carlos González ¹, Mauro Niño ^{1,*}  and Gustavo Ayala ²

¹ Departamento de Estructuras, Facultad de Ingeniería, UNAM, Mexico City 04510, Mexico; carlosecalva@gmail.com

² Instituto de Ingeniería, Coordinación de Ingeniería Estructural, UNAM, Mexico City 04510, Mexico; gayalam@ingen.unam.mx

* Correspondence: mninol@ingenieria.unam.edu

Abstract: Concerns about prolonged downtime and functionality losses observed after recent seismic events have made it clear that seismic design is heading towards a resilience-based approach. However, there is still currently no clear consensus on how to quantify and interpret resilience. In this document, a probabilistic approach to estimate recovery times and functionality loss in buildings is presented, which allows for the estimation of seismic resilience through consideration of delay times and the behavior of non-structural elements. To achieve these goals, simple models that associate structural response and the resilience parameters (recovery time and functionality) are defined. The proposed approach was implemented in a database for public school buildings in Puebla City, where the expected times and functionality were obtained, thus allowing for quantification of the seismic resilience of each structure. Furthermore, target values for low and high resilience are proposed, which helps to identify the weakest elements in the educative Mexican infrastructure. The results showed that the inclusion of delay times and non-structural elements in resilience quantification is mandatory if an overestimation of resilience values is to be avoided. At the same time, the target values allow for the different structures to be categorized according to the resilience values obtained, finding that a significant portion of Mexican school buildings are underprepared in a resilience context.

Keywords: seismic resilience; school buildings; vulnerability; functionality loss; community downtime



Citation: González, C.; Niño, M.; Ayala, G. Functionality Loss and Recovery Time Models for Structural Elements, Non-Structural Components, and Delay Times to Estimate the Seismic Resilience of Mexican School Buildings. *Buildings* **2023**, *13*, 1498. <https://doi.org/10.3390/buildings13061498>

Academic Editor: Giuseppina Uva

Received: 5 May 2023

Revised: 1 June 2023

Accepted: 7 June 2023

Published: 10 June 2023



Copyright: © 2023 by the authors. Licensee MDPI, Basel, Switzerland. This article is an open access article distributed under the terms and conditions of the Creative Commons Attribution (CC BY) license (<https://creativecommons.org/licenses/by/4.0/>).

1. Introduction

Seismic events throughout history have made it evident that creating non-collapsing structures is not enough to guarantee an acceptable post-earthquake scenario. This was observed during the 2017 earthquake in Mexico City, where a large part of the affected buildings showed no structural damage; however, the affected non-structural elements and contents caused an interruption to daily activities [1], affecting overall functionality, downtime, and resilience. The study of resilience in the context of earthquake engineering began with the definition of this concept [2]. This framework was then extended to propose different ways to characterize resilience with known parameters (time and functionality) so that it might be quantified [3,4]. This led to a framework to estimate resilience, as expressed in Equation (1).

$$R = \int_{t_0}^{t_{0E}} Q(t)/T_{LC} \quad (1)$$

where R is seismic resilience, T_{LC} is control time, $Q(t)$ is the time variant functionality curve which represents a non-stationary stochastic process, t_0 is the time of occurrence of the seismic event, and t_{0E} is the time at which target functionality is achieved.

Equation (1) has been adopted by numerous researchers in efforts to quantify the resilience of a particular system [5–7]. Several of these efforts are focused on lifeline infrastructure due to its high social relevance [4,8]; however, building infrastructure such as dwellings, schools, and hospitals is also important to maintain community resilience, as mentioned by Feng et al. [9] who studied the interdependency between different building sectors and its effects on community resilience. Particularly, school buildings have been the subject of several studies in terms of vulnerability, risk, and resilience. Examples are presented in Fontana et al. [10], who recognized the importance of non-lifeline infrastructure by assessing the seismic resilience of the educational sector in southern Italy, heavily focusing on a set of social factors that characterized the resilience. In addition, Ruggieri et al. [11,12] investigated the fragility, vulnerability, and risk of reinforced concrete (RC) school buildings in southern Italy with an emphasis on improving the simplified methods to assess the strength and post-earthquake state of such buildings.

Moreover, some other authors [5,7,13] have used methodologies englobing seismic hazards, structural modeling and analysis, seismic risk, and recovery functions to define a functionality curve and finally estimate resilience. In this regard, Anwar et al. [5] quantified seismic risk and sustainability as a function of repair costs, carbon emissions, and downtime using damage fragility and consequence functions of structural and non-structural components. Later, Samadian et al. [13] focused on estimating the seismic resilience of RC school buildings using vulnerability functions while taking into consideration the delay in repair times. Furthermore, Gonzalez et al. [7] defined expected annual resilience (EAR) using a methodology based on seismic risk, which takes into consideration the entire seismic environment affecting a certain structure. Recently, Gutiérrez and Ayala [14] proposed a probabilistic method to assess downtime and repair costs by considering the necessary manpower to achieve the restoration of buildings; nonetheless, the factors that delay the beginning of the repairing process were not considered.

Besides the quantification of resilience, another important yet somehow neglected aspect is the definition of target or acceptable values of downtime, functionality, and resilience. Some studies have proposed values for seismic resilience, such as those developed by Almufti et al. [15], who proposed that seismic resilience should be classified based on the structure's downtime. Furthermore, Mieler et al. [16] proposed a methodology where several community resilience targets are associated with the functionality of socially important systems (such as hospitals, schools, apartments, and power plants). However, both of the abovementioned proposals lack an analytical background. Hall and Giglio [17] emphasize the relevance of proper target resilience values and suggest that cost analysis may lead to optimal targets. Other researchers [18,19] that have oriented their efforts to propose a seismic resilience-based design have recommended target post-earthquake scenarios, such as Immediate Occupancy (IO), Rapid Recovery (RR), and Collapse Prevention (CP); nevertheless, there are no explicit discussions regarding the specific resilience or downtime values associated with such target scenarios.

Despite the current contributions, there are still opportunity areas in seismic resilience assessment and its interpretation. For instance, current studies present important simplifications such as estimating indirect losses as a fraction of direct losses [4,7] and the lack of a proper interpretation of the resilience values found [4,19]. For the above reasons, this paper presents a procedure to define expected recovery times, expected delay times, and expected functionality loss curves to be used in the seismic resilience assessment of buildings. Furthermore, an approach to define acceptable resilience values is also presented, which is intended to be useful in hazard prevention and decision making.

2. Methodology

This research presents a methodology to quantify resilience by estimating the parameters that compose the functionality profile, $Q(t)$, shown in Figure 1, where functionality can be seen as a function of time. In Figure 1, T_a refers to the time before the occurrence of an earthquake, where a gradual functionality decay can be seen due to aging and envi-

ronmental affections. This is followed by a functionality drop, FL, which occurs due to a seismic event, which is then followed by a flat region, Tb, which represents the delay time before the repair activities begin. Finally, in this representation, Tc and Td are the repair times for structural and non-structural elements, respectively.

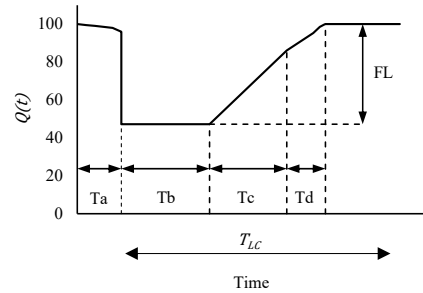


Figure 1. Functionality as a variable dependent on time in a post-earthquake scenario.

Estimation of each of the aforementioned components of the functionality profile, $Q(t)$, is associated with a parameter of structural response using an empirical model so that seismic resilience may be easily obtained. This is achieved with the method presented in Figure 2.

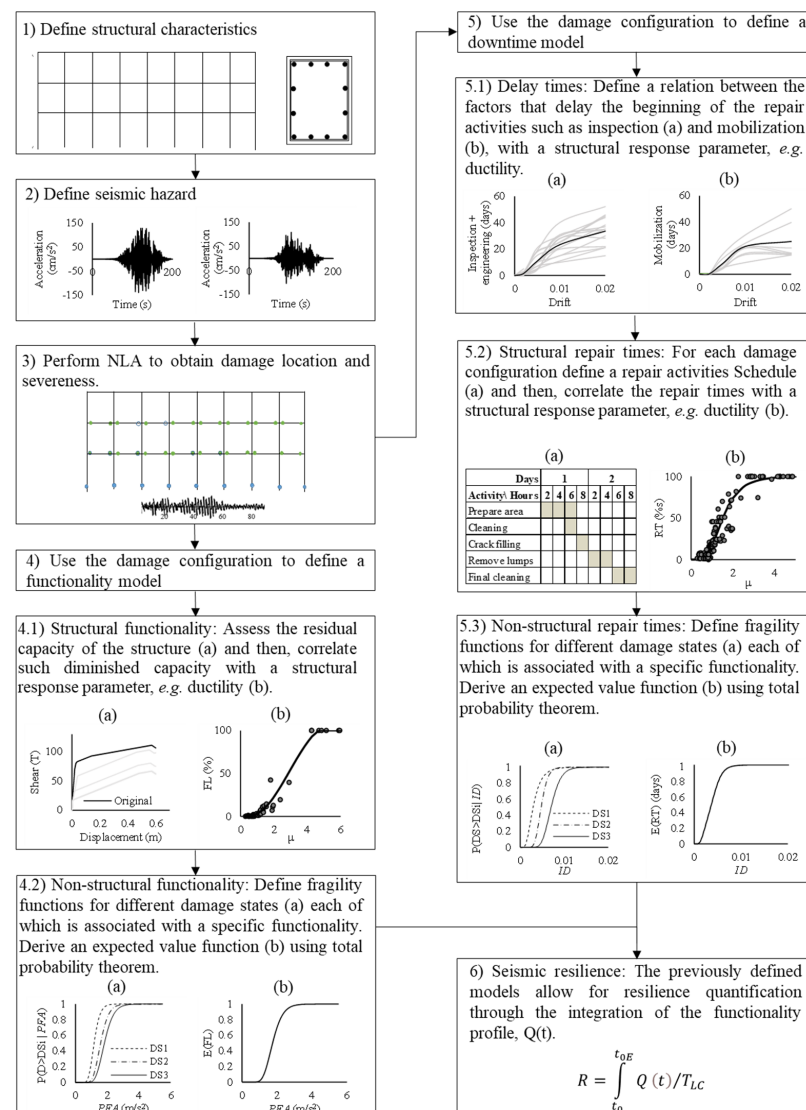


Figure 2. Methodology to define functionality and downtime models for quantifying seismic resilience.

In Figure 2, it is important to mention that steps 4 and 5 can be developed in parallel, both being necessary to perform step 6. In the following text, a brief description of every stage comprising the general methodology is presented.

2.1. Structural Characteristics

The characteristics of the structure, such as the plan and elevation geometry, section properties, and materials, must be obtained. If a particular infrastructure sector is studied, it is recommended to identify prototypes or archetypes so a wide range of existing buildings may be included in the same study.

2.2. Seismic Hazard

In this method, seismic hazard is defined through a set of seismic records representative of earthquakes with relevance to the study site. Such records are recommended to be taken from seismographic stations located in soil with similar characteristics to those existing in the study location.

2.3. Structural Analysis

Having defined the structural characteristics and the seismic hazard, a proper structural model can be created, followed by structural analysis where nonlinearity must be considered when studying global and local damage since it is a highly relevant component in the study of downtime and functionality loss. The nonlinear behavior can be conceived with hysteresis models such as the ones proposed by Ibarra et al. [20], which are particularly convenient for reinforced concrete modeling given the explicit considerations on the degradation of stiffness and strength properties due to cyclic loading, thus leading to a more realistic representation of structural behavior during an earthquake.

2.4. Functionality Loss

Functionality can be thought of as the measurement of how well a system performs a certain task. It is difficult to establish a general metric for functionality englobing all existing infrastructure as each single structure has a distinct function, e.g., power dams are designed to retain a certain volume of water while dwellings are meant to provide a living place for a certain amount of people. This was highlighted by Tsionis [21], who presented a collection of the metrics for functionality in different systems found in the literature. Some authors selected a particular functionality metric, as shown in [5] where the authors associated building functionality with its occupancy capacity using four stages for a post-earthquake scenario: IO (Immediate Occupancy), LF (Life Safety), CP (Collapse Prevention), and C (Collapse). On the other hand, some authors quantified functionality loss as the combination of both direct and indirect losses [4,13].

Despite the approaches currently developed, system functionality regarding buildings still needs further research since there are no consensual proposals on how to assess it. Therefore, in this study, a simple approach is proposed where functionality is considered as the contributions of both the structural and non-structural elements, as described below.

2.4.1. Structural Elements

A building is a structural system designed to provide a safe environment for the occupants, which is accomplished mainly due to its strength and stiffness properties. Thus, in this study, structural functionality is proposed to be measured based on integration of the seismic capacity of the system, as it is a parameter that may be measured before and after the occurrence of an earthquake and provides a clear estimation of the degradation of the properties of the overall system under study in terms of strength and stiffness. It is then proposed that the functionality loss of a structure be measured by quantifying the difference of the areas beneath the pre-earthquake (Figure 3a) and post-earthquake (Figure 3b) capacity curves.

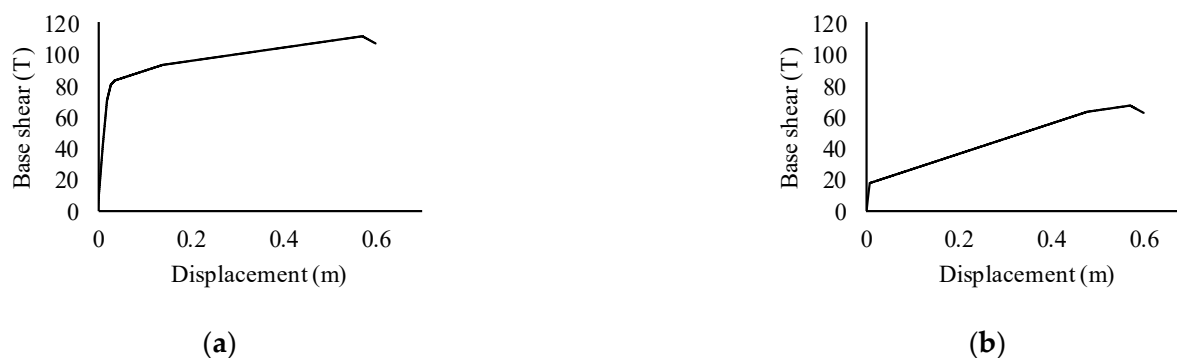


Figure 3. Static capacity curves: (a) original; (b) residual.

2.4.2. Non-Structural Elements and Contents

Those elements that despite having no contribution to gravitational or seismic load carrying capacity do have an influence on the daily operations of buildings are considered non-structural components. Such elements have a major contribution to the overall resilience of the structure since the presence of partial or total damage in them can cause an interruption to labor, hence diminishing functionality. Additionally, from a financial point of view, these elements are also important as they may represent up to 80% of the total building cost [22].

To estimate the contribution of the non-structural part to total functionality, it is proposed that expected functionality loss curves, $E(FL)$, be obtained for the non-structural elements of public school buildings in Mexico using the following procedure.

- Define the relevant non-structural elements and contents.
- Define models that correlate functionality loss and damage state.
- Generate fragility curves for all the damage states in each element.
- Obtain $E(FL)$ curves from the fragility functions.

On the other hand, contents themselves are elements that have no real continuity with the buildings; however, they are highly relevant to day-to-day operations. The abovementioned procedure can be applied to assess the contribution of a specific set of contents to the overall functionality and recovery times of a school building. Nevertheless, given the broad variety of existing contents in different schools, and to keep the results in a general state, the consideration of contents is beyond the scope of this research.

2.5. Downtime

Downtime is one of the main parameters required to characterize seismic resilience, which comprises repair and the delay times. The former refers to the required time to carry out the rehabilitation activities for the damaged structural and non-structural components, while the latter refers to all the factors that delay the beginning of the repair activities; this parameter includes inspection of structural damage, engineering activities, restoration of services, funding recollection, and mobilization [15].

2.5.1. Delay Time Factors

Indirect losses caused by downtime are commonly associated with impediments to providing certain services or producing certain products due to functionality loss in the infrastructure. It is common that these losses represent a large percentage of the total economic losses caused by an earthquake, particularly in commercial buildings [1,23]. This is why downtime must be properly estimated where delay factors have an important role and is the reason why it has been explored in the past by many authors, e.g., [1,15,24], with the framework proposed by Almufti et al. [15] being the most widely adopted. This framework comprises the following factors delaying the repair activities required to bring back the lost functionality:

- Visual inspection: after the occurrence of an earthquake, structures require an inspection, which may be superficial in the case of light or no damage or deep in the case of severe damage.
- Engineering: if the structure is moderately or severely damaged, it is necessary to carry out an engineering process to ensure that safety and functionality are recovered by means of the repairing actions.
- Permits: Permit approval from the local building jurisdiction would likely be required for buildings that exhibit structural damage. Repairs of certain non-structural components may also require permits, but these may usually be obtained “over the counter” and do not account for significant delays.
- Financing: Significant delays may occur due to the inability to obtain financing to fund the necessary repairs. Financing may be procured through loans or insurance payments. Federal or other government grants should not be considered a viable financing option due to the uncertainty in securing these funds.
- Contractor mobilization: there are several factors that are critical contributors to the overall time required to mobilize a contractor, including a shortage of contractors, the severity of damage, bidding, essential facilities, and building height.

Figure 4 shows a representation of the time consumed by the delay factors. It should be noted that some of them may be performed at the same time (parallel); hence, the total delay time would be the path that yields the maximum time.

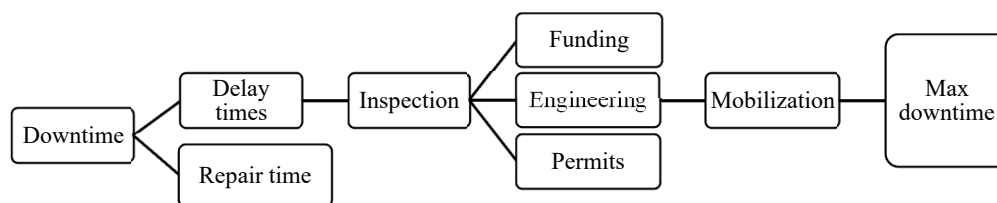


Figure 4. Delay time parameters.

Estimation of the delay time parameters must be performed while trying to keep both simplicity and rationality; therefore, in this research, it is proposed that structural damage is related to the delay time parameters, such as the inspection, engineering, and mobilization times. The average time associated with each damage state (DS) will be different for every socioeconomic environment and can be obtained through data analysis from historic records or from stipulations on general codes or literature. For example, Alcocer et al. [25] indicate that partial inspections (which are applied to slightly damaged structures) in Mexican school buildings should not take more than 30 min. Furthermore, recognizing that the delay times due to funding and permits involve several socioeconomic variables, these times are recommended to be estimated either from government-issued specifications or from historical data related to past earthquakes.

2.5.2. Repair Times in Structural Elements

As previously mentioned, repair times involve all the required procedures to take damaged infrastructure to a target undamaged level. Those actions are defined based on the experience of engineers and are dependent on the construction material, the available resources, and the type of damage, among other factors. Considering this information, construction experts develop work schedules enlisting proper rehabilitation activities, as well as the interdependence of such activities.

If a particular structure is being studied, it is reasonable to eliminate the material type and available resources as variables and estimate the repairing times solely based on the physical damage to the structure. By studying typical rehabilitation techniques, it is then possible to define suitable work schedules. Particularly for Mexican reinforced concrete structures, the use of epoxy resins to repair columns with minor damages due to earthquake actions is commonly accepted, considering that it would allow for the original earthquake

resistant capacity to be reached in a reasonable manner. The jacketing of concrete (resulting in an increase in the section and the reinforcement) is generally employed when damage in columns is moderate or severe [26]. Thus, with this information and the data regarding the amount and location of damage, the repair times associated with structural elements can be estimated. Additionally, it is important to notice that the abovementioned repairing process is related to structural damage due to seismic forces, and differential settlement-related damage is not considered due to being out of the scope of this research.

2.5.3. Repair Times in Non-Structural Elements

To estimate the contribution of the non-structural part to total downtime, it is proposed that expected time curves, $E(RT)$, be obtained from fragility functions for the non-structural elements of public school buildings in Mexico in a similar manner to the procedure used to obtain the expected non-structural functionality loss:

- Define the relevant non-structural elements and contents.
- Define models that correlate repair time and damage state.
- Generate fragility curves for all the damage states in each element.
- Create $E(RT)$ curves.

2.6. Seismic Resilience

Steps 2.4 and 2.5 describe the procedure to obtain empirical models that correlate the structural response with functionality loss and downtime. Such models can then be applied to process the results of nonlinear analysis in terms of the parameters that compose Equation (1) and then quantify seismic resilience, which represents the average functionality over a predefined time, named control time, of a system that has been subjected to damage due to a seismic event.

3. Results

Given their high social relevance, public school buildings are important structural systems that require study. For this reason and given the high seismicity in the state of Puebla, in addition to the poor performance of such buildings [27], the school buildings located in the state of Puebla, Mexico, were studied in this paper. The studied schools were represented by the typologies depicted in Figure 5, where buildings from one to three stories with a single 8-m bay in the transversal direction and eight 3 m bays in the longitudinal direction, are shown. Such typologies were selected according to the archetypes of Mexican public school buildings, defined in the technical guide for seismic rehabilitation of school buildings in Mexico City and by the National Institute of Educative Infrastructure (INIFED, for its acronym in Spanish) [26]. Additionally, two years of construction were selected to represent a large portion of the currently working educative institutions in Mexico (1996 and 2008). The structural system consists of reinforced concrete frames. A database containing the currently active education institutions with the aforementioned typologies was employed (Figure 6).

Given the regularity in the planning and elevation of real educative buildings, it is reasonable to represent the structural models as 2D frames with the aforementioned geometries (Figure 5). Such models were developed in OpenSees [28] considering 5% damping with respect to the critical value. As the modification in the period and the damping ratio associated with soil–structure interaction (SSI) may be beneficial [29,30], and due to the fact that the effects of SSI are less significant in low-rise structures [31], fixed bases and no SSI effects were considered. Damage is considered through a concentrated plasticity model with plastic hinges at the ends of elastic structural elements, which is achieved using a modified Ibarra–Medina–Krawinkler hysteresis model [20] that conveniently allows for the degradation of stiffness and strength properties due to cyclic loading to be taken into consideration. Figure 7 displays reinforcement arrangement for some of the 2008 structures; 1996 structures were not included to maintain conciseness. Furthermore, Figure 8 shows moment–curvature relationships for the displayed sections; such diagrams were used in

the definition of the backbone for the hysteresis model. It should be noted that section analysis was conducted considering the short dimension of the rectangular columns, since that is the relevant orientation according to the 2D frame proposed.

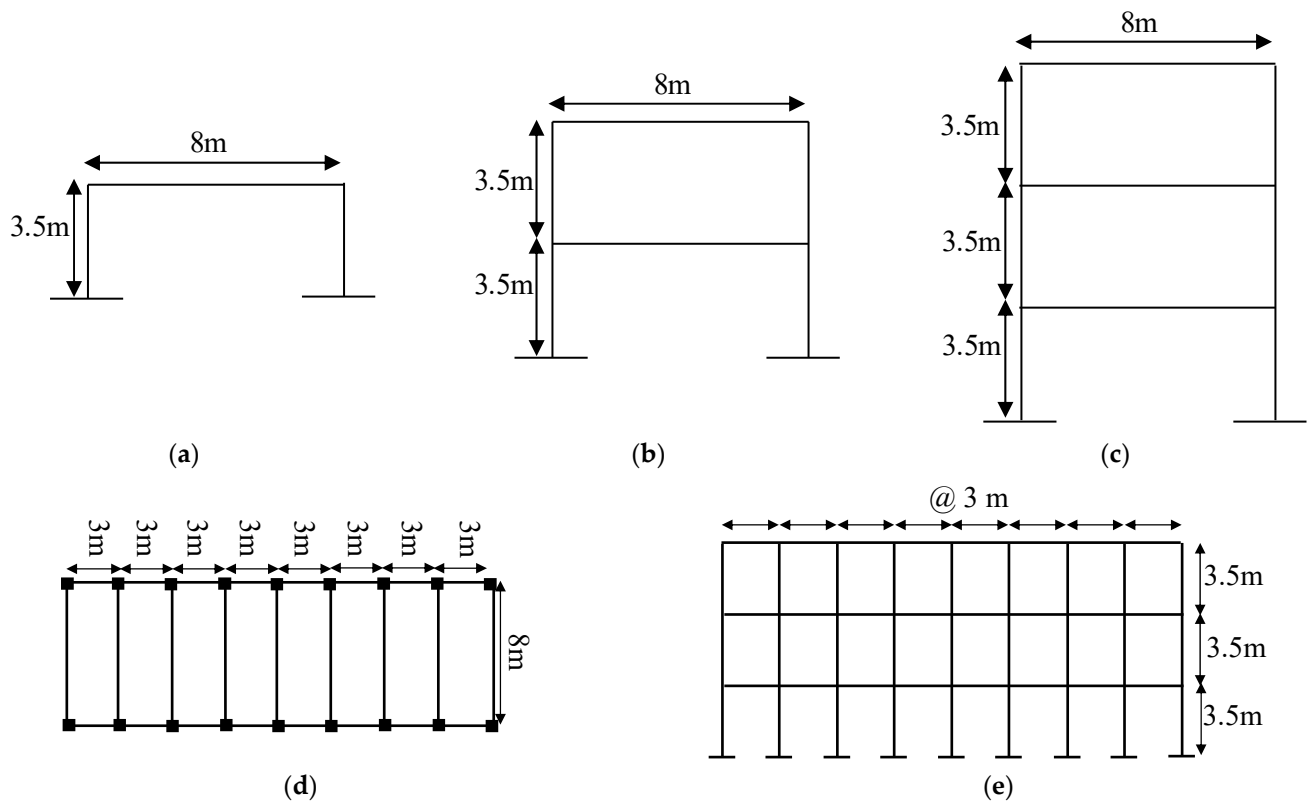


Figure 5. Different geometries of the studied buildings: (a) single-story building, (b) two-story building, (c) three-story building, (d) plant view, (e) lateral view of a three-story building.

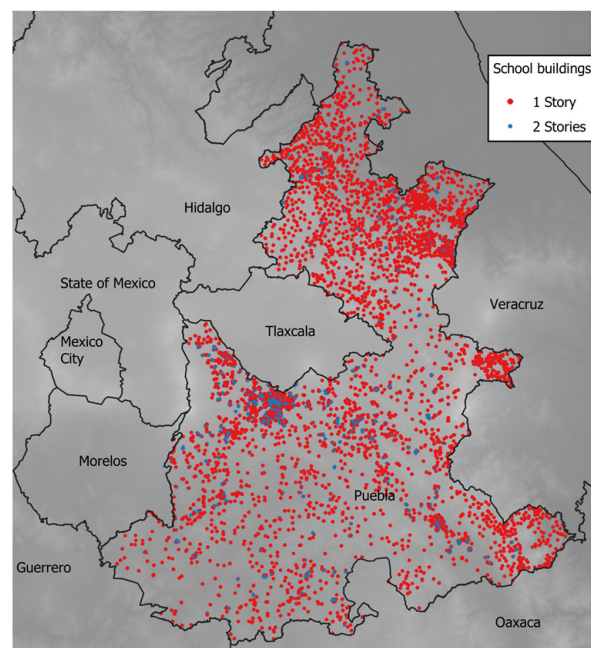
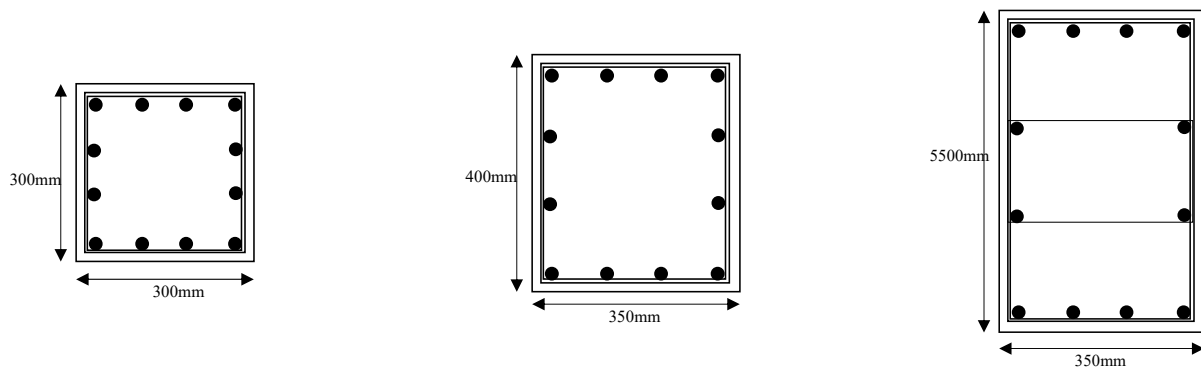


Figure 6. Location of current school buildings in the state of Puebla.



Twelve vars with a theoretical diameter of 19.6 mm, with 9.55 mm diameter stirrups with a spacing of 75 mm. (a)
 Twelve vars with a theoretical diameter of 22.8 mm, with 9.55 mm diameter stirrups with a spacing of 87.5 mm. (b)
 Twelve vars with a theoretical diameter of 23 mm, with 9.55 mm diameter stirrups with a spacing of 87.5 mm. (c)

Figure 7. Reinforcement arrangement for elements in the 2008 structures: (a) columns in single-story structures, (b) columns of the second story of the two-story structures, and (c) columns of the first story of the three-story structure.

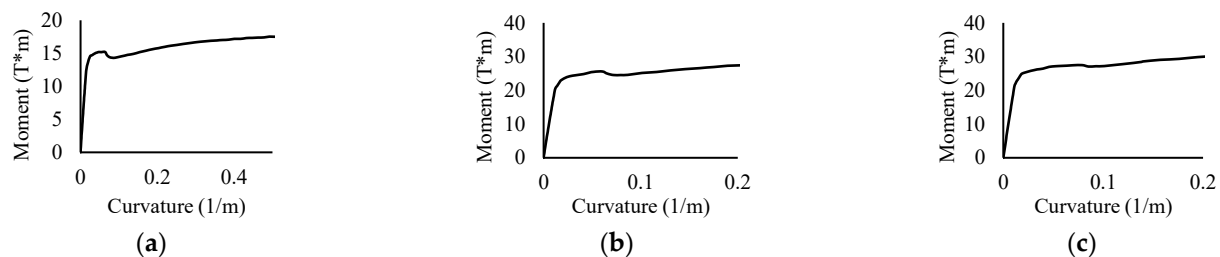


Figure 8. Moment–curvature relationships for elements in the 2008 structures: (a) columns in single-story structures, (b) columns of the second story of the two-story structures, and (c) columns of the first story of the three-story structure. Analysis performed in the short direction of the sections.

To assess the potential damage on the structures, incremental dynamic analysis (IDA) [32] and nonlinear time history analysis (NLTHA) were performed on each structure using OpenSees [28] and 98 different seismic records obtained from accelerometric stations located in firm soil (Table 1). Such records were selected since the soil characteristics in the location of each station are similar to the dominant period of the study sites. Furthermore, the records shown in Table 1 are associated with earthquakes that occurred in seismic sources that have historically affected the study site. Figure 9 presents the IDA results for the different studied archetypes in terms of maximum displacement since it is the most relevant for the estimation of ductility, which will be used for definition of the empirical models that correlate resilience parameters with structural response.

Table 1. Seismic records used for the nonlinear analysis (NLA) of structures obtained from stations located in hard soil.

Station	Date (d/m/y)	Direction	Epicenter		Mw	Station	Date (d/m/y)	Direction	Epicenter		Mw
			Lat(°)	Lon(°)					Lat(°)	Lon(°)	
ARTG	14/01/91	EW-NS	17.86	101.8	5.2	COYC	19/07/97	EW-NS	15.86	98.26	6.7
ARTG	11/06/86	EW-NS	15.14	93.51	5.8	COYC	19/09/85	EW-NS	18.41	102.4	8.1
ARTG	05/01/90	EW-NS	18.71	107.0	5.8	COYC	20/09/85	EW-NS	17.82	101.6	7.6
ARTG	30/04/86	EW-NS	18.36	103.0	7.0	COYC	22/03/97	EW-NS	17.04	99.76	4.7
CALE	11/01/97	EW-NS	18.34	102.5	7.1	COYC	25/04/89	EW-NS	16.58	99.46	6.9
CALE	19/09/85	EW-NS	18.41	102.4	8.1	COYC	30/09/99	EW-NS	16.05	97.0	7.4

Table 1. Cont.

Station	Date (d/m/y)	Direction	Epicenter		Mw	Station	Date (d/m/y)	Direction	Epicenter		Mw
			Lat(°)	Lon(°)					Lat(°)	Lon(°)	
CALE	22/05/97	EW-NS	18.41	101.8	6.0	CSER	15/05/93	EW-NS	16.47	98.72	6.0
CALE	05/01/90	EW-NS	18.71	107.0	5.8	CSER	15/06/99	EW-NS	18.13	97.53	7.0
CALE	30/04/86	EW-NS	18.36	103.0	7.0	CSER	16/09/89	EW-NS	16.21	94.01	5.9
CENA	15/06/99	EW-NS	18.13	97.53	7.0	CSER	23/02/94	EW-NS	17.82	97.30	5.4
CENA	30/09/99	EW-NS	16.05	97.0	7.4	CSER	25/04/89	EW-NS	16.58	99.46	6.9
COPL	14/09/95	EW-NS	17.00	99.00	7.3	CSER	30/09/99	EW-NS	16.05	97.0	7.4
COPL	15/06/99	EW-NS	18.13	97.53	7.0	CUER	10/12/94	EW-NS	18.02	101.56	6.2
COPL	21/01/97	EW-NS	16.44	98.15	5.6	CUER	14/09/95	EW-NS	17.00	99.00	7.3
COPL	24/10/93	EW-NS	16.76	98.76	6.6	CUER	15/06/99	EW-NS	18.13	97.53	7.0
COPL	25/04/89	EW-NS	16.58	99.46	6.9	CUER	23/05/94	EW-NS	17.97	100.6	5.8
COPL	30/09/99	EW-NS	16.05	97.0	7.4	CUER	30/09/99	EW-NS	16.05	97.0	7.4
COYC	07/06/98	EW-NS	15.82	94.07	6.2	RIPC	14/09/95	EW-NS	17.00	99.00	7.3
COYC	05/07/98	EW-NS	16.83	100.1	5.2	RIPC	23/02/94	EW-NS	17.82	97.30	5.4
COYC	08/05/97	EW-NS	17.32	100.4	5.1	SXPU	19/09/85	EW-NS	18.41	102.4	8.1
COYC	11/01/97	EW-NS	18.34	102.5	7.1	SXPU	20/09/85	EW-NS	17.82	101.6	7.6
COYC	14/09/95	EW-NS	17.00	99.00	7.3	YAIG	15/06/99	EW-NS	18.13	97.53	7.0
COYC	15/06/99	EW-NS	18.13	97.53	7.0	YAIG	30/09/99	EW-NS	16.05	97.0	7.4

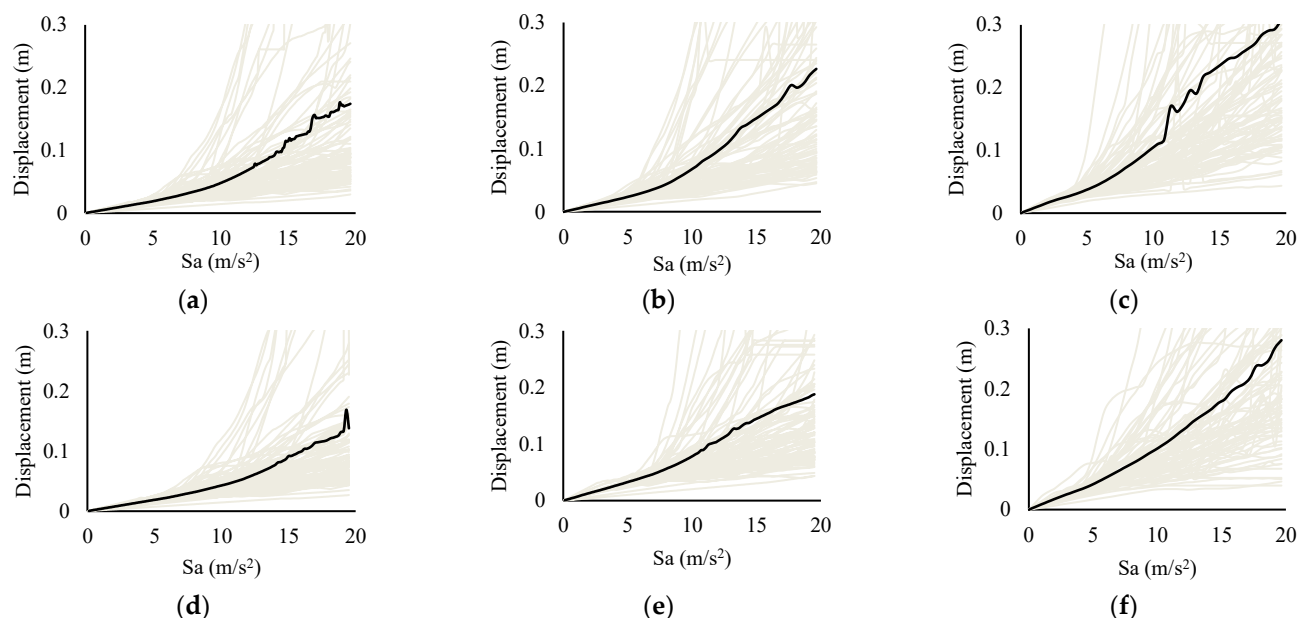


Figure 9. IDA displacement curves: (a) single-story 1996; (b) single-story 2008; (c) two-story 1996; (d) two-story 2008; (e) three-story 1996; (f) three-story 2008. Grey lines represent the response for particular seismic records, and black lines the mean values.

Results of NLTHA were analyzed in terms of the plastic hinge rotations of each element and their relationship with global maximum displacement, where every bar or column in Figure 10 represents the result of a single analysis associated with a particular seismic record. It can be seen that there is an increasing relation between the maximum displacements and the appearance of plastic hinges. It can also be observed that, in general, plastic hinges first appear at the ends of beams (according to Table 2), particularly on the first floor. This may be attributed to the strong column–weak beam model.

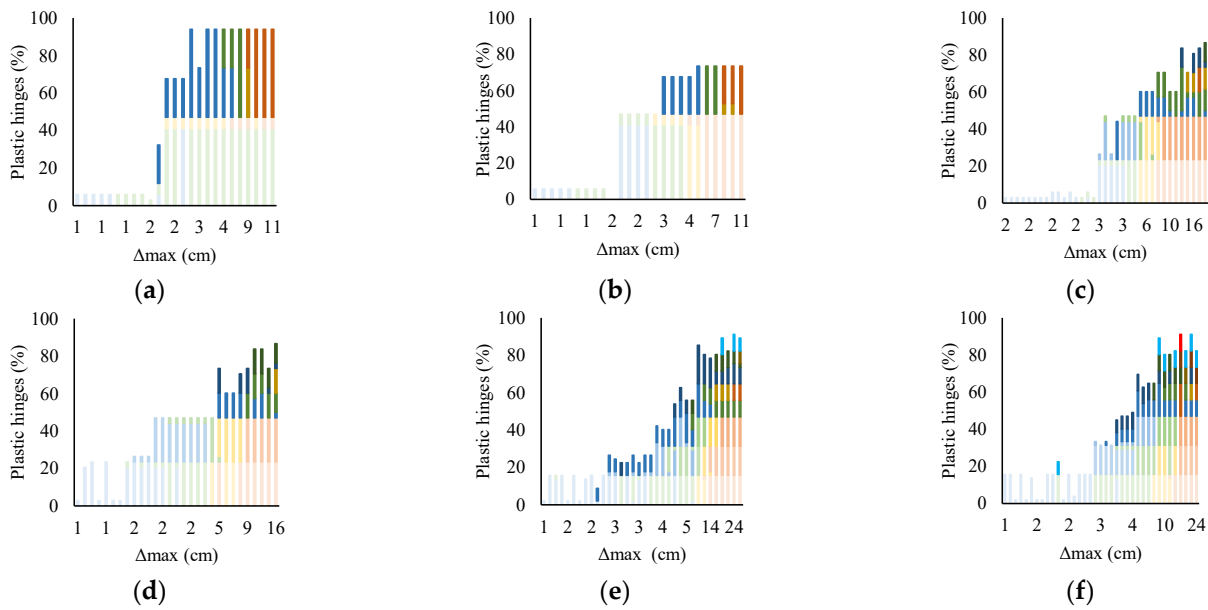


Figure 10. Percentage of plastic hinge rotations for a given displacement: (a) single-story 1996; (b) single-story 2008; (c) two-story 1996; (d) two-story 2008; (e) three-story 1996; (f) three-story 2008.

Table 2. Classification according to the location and magnitude of plastic hinges.

Color	Location Beams	Color	Location Beams	Color	Location Beams	Color	Location Columns	Color	Location Columns	Color	Location Columns	DS
[Light Blue]	Floor 1	[Light Blue]	Floor 2	[Light Blue]	Floor 3	[Dark Blue]	Floor 1	[Dark Blue]	Floor 2	[Light Blue]	Floor 3	DS1
[Light Green]	Floor 1	[Light Green]	Floor 2	[Light Green]	Floor 3	[Dark Green]	Floor 1	[Dark Green]	Floor 2	[Light Green]	Floor 3	DS2
[Light Yellow]	Floor 1	[Light Yellow]	Floor 2	[Light Yellow]	Floor 3	[Dark Yellow]	Floor 1	[Dark Yellow]	Floor 2	[Light Yellow]	Floor 3	DS3
[Light Orange]	Floor 1	[Light Orange]	Floor 2	[Light Orange]	Floor 3	[Dark Orange]	Floor 1	[Dark Orange]	Floor 2	[Light Orange]	Floor 3	DS4

To study the general tendency between displacement and damage location considering all the structures studied, the previous results were combined and displacement then normalized to each individual yield displacement, obtaining the model of Figure 11, where the percentage of plastic hinges is related to the ductility demand, μ . Results presented in the aforementioned figure allow for damage state to be inferred in any of the analyzed structures, given the structural response in terms of ductility when subjected to earthquake loading. Low ductility values are associated with few lightly damaged elements, which is hypothesized to be related to small downtime and functionality loss. On the other hand, high ductility demand is associated with severe damage in various elements, with prolonged downtime and a high loss of functionality thus to be expected. This is expanded in the following sections.

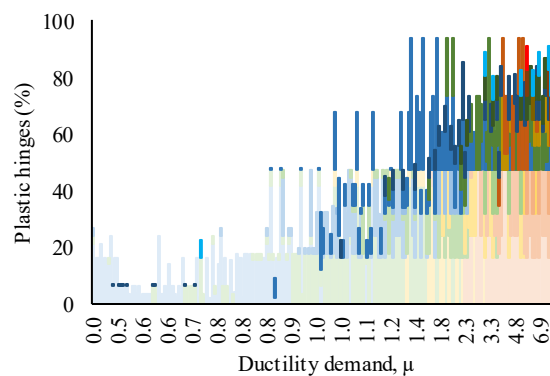


Figure 11. Percentage of plastic hinge rotations for a given ductility demand for all the analyzed structures.

3.1. Expected Functionality Loss Curves

As previously stated, structural functionality loss is calculated as the difference in the integrals of the original and residual capacity curves; therefore, it is necessary to obtain the original push-over curve and then push-over curves for each cumulative damage state generated by a particular seismic record. To achieve this goal, it is necessary to define stiffness and strength degradation in damaged elements, which can be achieved by considering residual strength and stiffness factors according to the damage state in a certain element. When assessing the state of structural elements in existing buildings, methods such as the one proposed by Forte et al. [33] are recommended; however, in order to maintain consistency with local standards, in this study, the considerations proposed in the Code for Seismic Rehabilitation of Damaged Concrete Buildings [34] were adopted. If an element presented light damage, 1.0 and 0.75 strength and stiffness factors were considered. On the other hand, when there was moderate damage, those factors were 0.75 and 0.5. Finally, when there was severe damage, both factor values were 0.0. Once the residual properties of each element were defined, push-over analysis with damaged elements was performed for each seismic record and each structure. The capacity of the complete structural system was then assessed through the area beneath the capacity curve (Figure 12). The difference between the undamaged structure (black line) and the damaged scenarios (grey lines) is the structural functionality loss.

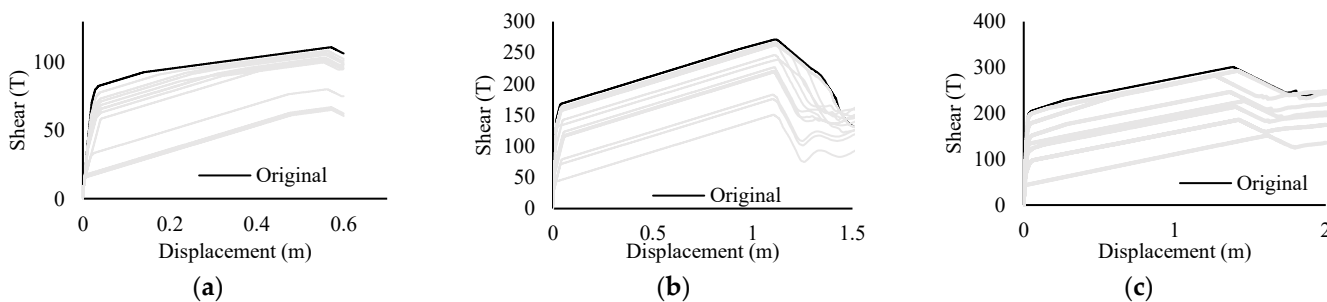


Figure 12. Capacity curves for (a) one-story, (b) two-story, and (c) three-story structures.

Each value of functionality loss is then associated with a ductility demand value, μ , and plotted, as shown in Figure 13.

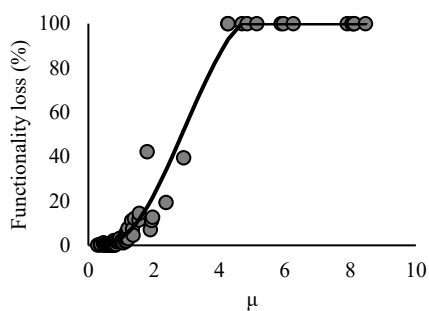


Figure 13. General functionality loss model.

Finally, through regression analysis, a generalized functionality loss model is defined, which is depicted in Equation (2).

$$FL = \alpha \beta^{\left(\frac{1}{\mu}\right)} \mu^\gamma \tag{2}$$

where α , β , and γ are dimensionless factors with values of 6.0, 0.54, and 3.66, respectively.

With the above equation, results from performing IDA were processed to obtain pseudo-acceleration (S_a) vs. functionality loss curves for every used seismic record (grey lines in Figure 14), as well as the mean value (solid black line) and the standard deviation (dashed line). The mean value corresponds to the expected functionality loss curve.

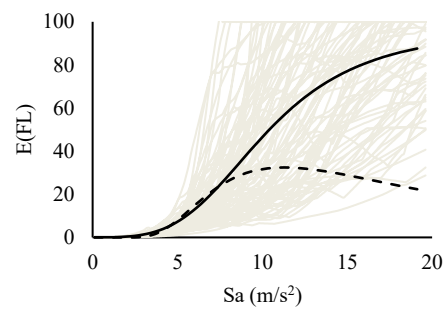


Figure 14. Functionality loss curves and their mean value.

3.2. Downtimes: Delay Time Estimation

To take into consideration the possible delays in the beginning of repair activities, time related to inspection, engineering, and mobilization was estimated and related to a measure of structural damage in the form of global drifts. This is important since drifts can be related to damage states, as proposed in FEMA [35].

To estimate the mentioned times, the available literature was employed [15,25,36], as well as the expert opinions of professionals with experience in post-earthquake damage assessment in Mexico. In such research, the approximate times associated with light, moderate, and severe damage were studied, and although there is a large dispersion within the gathered data, an increasing correlation exists between global drift and delay times (Figure 15).

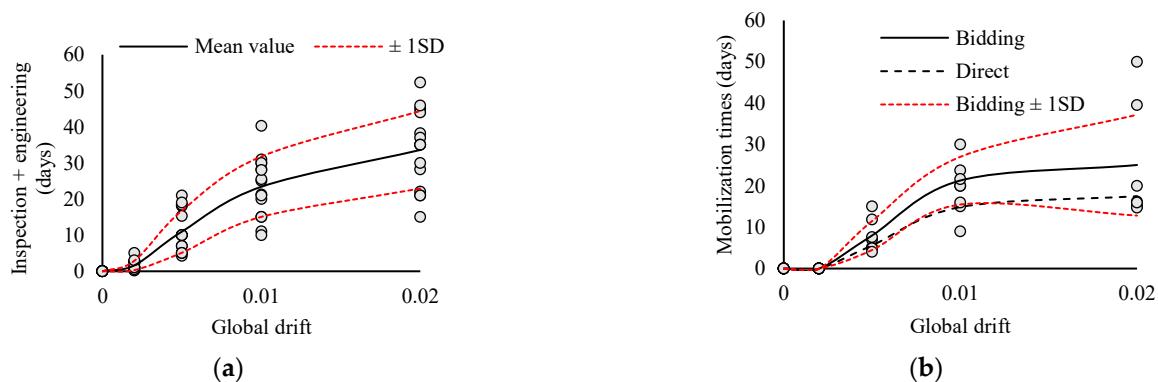


Figure 15. Delay time curves: (a) inspection and engineering; (b) mobilization times as a function of global drift.

It can be noted in Figure 15a that small global drifts, which mean that little or no damage has occurred, are related to minimum inspection and engineering times; however, as damage increases, elements require more detailed inspection, resulting in a greater amount of calculation and engineering activity. In a similar manner, Figure 15b shows that mobilization time increases along with increased structural response (global drift). In this particular case, two situations are presented, the first of which is a traditional bidding process, which is the most time-consuming factor in the mobilization (solid line in Figure 15b), and the second of which is an approach considering direct assignment of the rehabilitation project (dashed black line in Figure 15b).

Direct assignment leads to less mobilization time, which will have an impact on the resilience value. Equations (5) and (6) were obtained from nonlinear regression analysis and show expressions for inspection–engineering ($I-ET$) and mobilization (MT) as a function of global drifts (Drift), where, A , B , C , and D are dimensionless factors taking values of -0.15 , 0.00007 , 34.63 , and 1.97 , respectively, while θ , η , γ , κ are factors with values of 23.72 , 3.34 , and 0.0063 , respectively.

$$I-ET = \frac{AB + CD_{drift}^D}{B + D_{drift}^D} \quad (3)$$

$$MT = \frac{\theta D_{rift}^{\eta}}{\kappa^{\eta} + x^{\eta}} \quad (4)$$

Furthermore, in Figure 15, the mean value ± 1 standard deviation (1 SD) for both charts is also presented, where it can be seen that inspection and engineering times have a 70% confidence interval of being within ± 1 SD. On the other hand, mobilization times have an 80% confidence interval of being within ± 1 SD.

When combining the models shown in Figure 15a,b with the results of the IDA, inspection, engineering, and mobilization times can be presented as a function of ground motion intensity (S_a), as observed in Figure 16. Grey lines represent the results for each individual seismic record, while the medium values of the curves shown in Figure 16 are the expected inspection and engineering times, $E(I-ET)$ (solid black line in Figure 16a), and the expected mobilization times with bidding, $E(MT)$ (solid black line in Figure 16b), with the standard deviation represented by a dashed line for both functions.

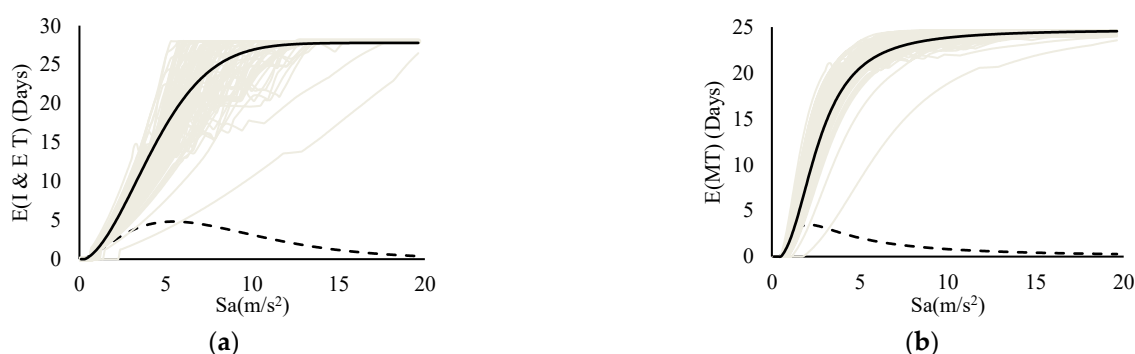


Figure 16. Expected time functions for (a) inspection and engineering time and (b) mobilization time with bidding.

Finally, information regarding permits and funding was obtained from the INIFED [37], indicating that, as a part of the implemented strategies for damage assessment and contingency, resource management involves presenting the proper requisitions to the government ministry informing them of the needed resources and a scheme of the rehabilitation actions. This process is estimated to last 7 days. The government ministry then reviews, verifies, and issues a response to the solicitation in an estimated time of 2 days [37].

3.3. Expected Repair Time Curves

One of the advantages of processing the results as shown in Figure 11 is the ability to be able to estimate repair schedules for each value of μ reached according to the severities and associated locations of plastic hinges.

Since a certain plastic hinge magnitude reflects a physical damage state, repair programs can then be developed by engineers with expertise in post-earthquake repairing processes, taking into consideration typical manpower in Mexico and a post-earthquake scenario. Some examples of these repair schedules are shown in Figure 17.

Taking into account an increment in efficiency when repairing multiple damaged elements, global repair times were estimated for each structure and each seismic event with the aim of achieving a generalized model for all the structures under study. To achieve this goal, normalization was performed by obtaining the ratio of each individual repair time divided into the maximum possible repair time on each structure.

Figure 18 displays the results obtained from the conversion of damage to recovery time (RT), where good agreement between the results and the proposed regression model is observed, mainly for values of μ less than 2. Furthermore, the model is given by Equation (5), where a , b , and c are dimensionless adjustment factors with values of 101.45,

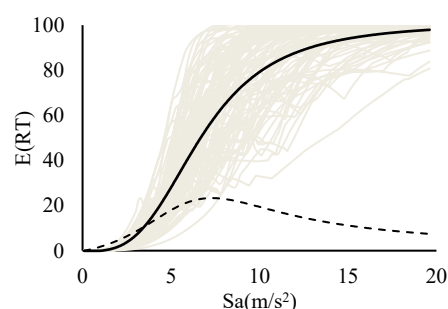


Figure 19. Process to obtain expected repair time functions.

3.4. Non-Structural Elements

School buildings may be particularly vulnerable to the failure of non-structural elements and contents. A study carried out by González et al. [7] showed that life safety in Mexican school buildings is mostly threatened by the failure of non-structural elements; therefore, the response of such elements must be controlled. In that sense, it is proposed in this paper that global resilience be used as the parameter to evaluate the response of those elements.

According to the National Institute for Education Assessment (INEE for its acronym in Spanish) [38], basic furniture requirements and teaching equipment must include student and teacher desks, teachers' chairs, blackboards, shelves, luminaires, ceilings, floors, water dispensers, windows, and sewer systems. Among the above elements, this study considers windows, luminaries, and ceilings as the most relevant to resilience, as indicated by a group of engineers in agreement with teachers and the administrative staff of educational institutions. Additionally, as approximately 95% of the schools in Mexico have either concrete or masonry walls, it is necessary to take them into consideration as well.

In the absence of information specific to the Mexican context, the repair time for each of the elements previously mentioned was obtained from the Federal Emergency Management Agency (FEMA) database Performance Assessment Calculation Tool (PACT) [39]. Although the different socioeconomic environment between the U.S. and Mexico may lead to different estimated repair times, it is considered a good first approximation with the available data. Table 3 shows an example of repair measures and repair times for different damage states for generic window glass (monolithic with unspecified layer characteristics, an aspect ratio of 6:5, and no further specifications).

Table 3. Repair times for different damage states in a window glass piece (adapted from FEMA [39]).

Damage State	Physical Damage	Recommended Repair	Repair Time (Days)
DS1—Light damage	Sealer failure	Remove the glass piece to repair the sealer.	0.68
DS2—Moderate damage	Window cracking	Replace the cracked glass piece.	1.02
DS3—Severe damage/Collapse	Window collapse	Replace the glass piece and temporarily cover the gap.	1.5

Fragility curves for each non-structural element and each damage state were then obtained. This can be achieved by empirical methods, analytical methods, or by consulting the available literature [40,41]. In this study, the available data in the PACT were employed, where fragility functions for different damage states are provided. The collected curves are presented in Figure 20, where it may be seen that walls and windows are associated with maximum inter-story (*ID*) drift, while ceilings and luminaires are sensitive to peak floor acceleration (*PFA*).

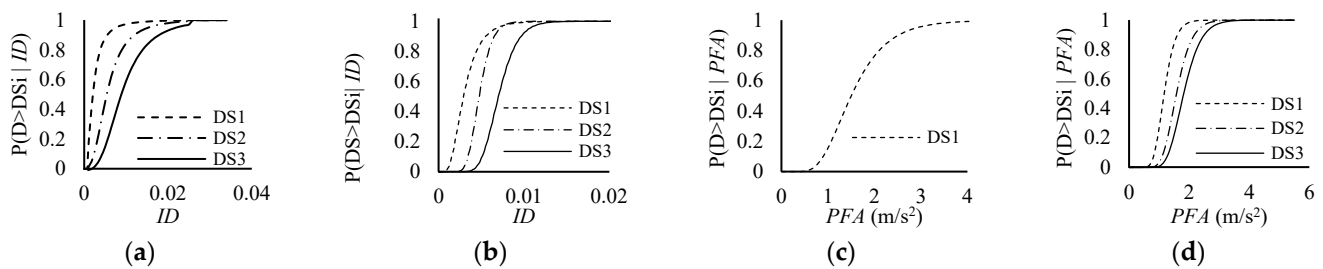


Figure 20. Fragility functions for different damage states in (a) walls, (b) windows, (c) luminaires, and (d) ceilings.

As previously stated, the previous fragility curves are associated with different damage states, each of which is related to a mean repair time (see Table 3); hence, expected repair times and functionality loss curves can be deduced by using Equation (6).

$$E(P) = \sum_{j=1}^{NDS} E(P|DS_j) \cdot \Pr(DS_j|ID \text{ or } PFA) \quad (6)$$

where NDS is the value for repair times or functionality values, $E(P|DS_j)$ is the mean repair time observed given damage state DS , and $\Pr(DS_j|ID \text{ or } PFA)$ is the probability of occurrence of a time or functionality given a certain ID or PFA value. The expected non-structural repair times, $E(RT)$, and expected non-structural functionality loss curves, $E(FL)$, are presented in Figure 21.

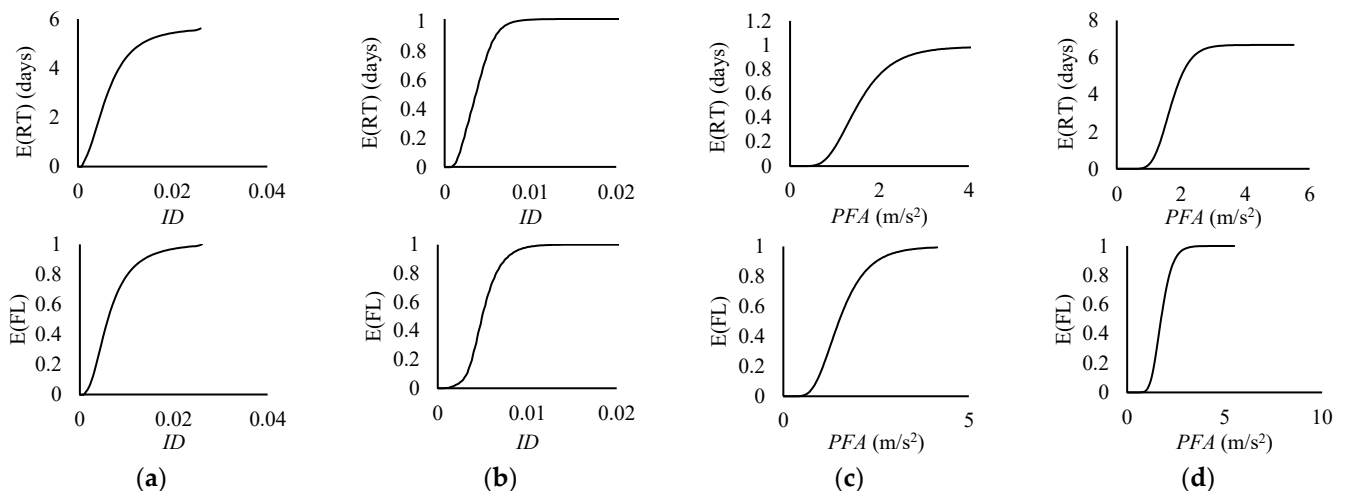


Figure 21. Expected curves for non-structural elements: (a) walls, (b) windows, (c) luminaires, (d) ceilings.

3.5. Seismic Resilience

In this research, seismic resilience is estimated through Equation (1) as a parameter to assess the overall ability of a building and its components to sustain earthquake-induced damage and return back to a pre-earthquake condition within a certain time. As mentioned previously, seismic resilience-related research often uses simplifications, such as not considering the delay time nor behavior of the non-structural elements. To highlight the implications of these assumptions, different approaches for resilience quantification are considered in this paper: a simple approach with no delay times and without non-structural elements (Figure 22a,b), an approach considering delay times (Figure 22b,c), and a refined approach using both delay times and non-structural elements (Figure 22c). Equation (1) is used to estimate resilience on each of the abovementioned approaches.

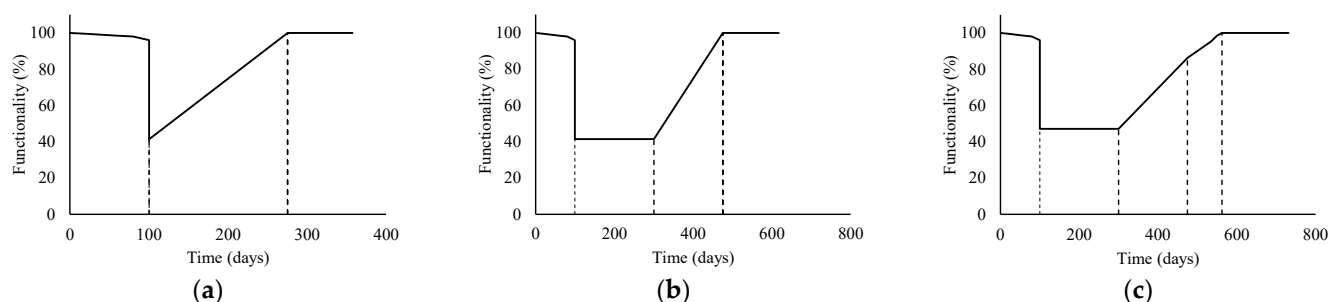


Figure 22. Seismic resilience considering the (a) simple approach, (b) the approach considering delay times, and (c) the approach considering delay times and non-structural elements.

4. Discussion

4.1. Application of the Expected Times and Functionality Curves

Resilience was estimated for a large database of Mexican school buildings located in the state of Puebla given its high seismic activity. To this end, seismic hazard was defined using the spectral pseudoacceleration (S_a) associated with the fundamental vibration period of each structure, which considered 5% damping with respect to the critical value as the intensity measure. Ground motion intensity was represented as a random variable by its first two probabilistic moments: (1) mean value and (2) variance. Ground motion prediction equations were used to evaluate the influence of each source on the observation site. In addition, intensity was treated as a random variable with log-normal distribution, where the mean is expressed as a function of the magnitude of the earthquake and the distance between the source and the site. Further information regarding the seismic hazards associated with this research can be found in the References section [41].

The CAPRA [42] software for risk analysis is commonly used to compute risk in terms of expected annual loss or probable maximum loss using vulnerability curves (or expected loss); however, in this study, it was useful in obtaining the expected downtimes and expected functionality loss and was used to carry out several analyses, where, instead of using vulnerability information, the expected functionality loss and downtime models previously developed (Figures 14 and 16) were used.

Table 4 shows the results for the repair times (RT_S) and functionality losses (FL_S) of structural elements. Additionally, values for repair times and functionality loss in walls (RT_M and FL_M , respectively), windows (RT_W and FL_W), luminaries (RT_L and FL_L), and ceilings (RT_C and FL_C) are presented for a single school building located in a high seismicity zone in Puebla City considering seven critical scenarios which were selected according to the severeness of their consequences and occurrence frequency. The repair time values are normalized to the maximum possible repair time to achieve compatibility with the structural repair times model proposed (Figure 18). Additionally, expected delay times are also presented to take into account inspection and engineering times (I&ET) and mobilization times for both bidding (MT(B)) and direct assignation of the repair activities (MT(D)). When using direct assignation, the delay times due to mobilization can be reduced by up to 39%, which is expected to have an impact on resilience.

Table 4. Repair times and functionality loss for structural and non-structural elements and delay times.

Magnitude	Frequency	RT_S	FL_S	RT_M	FL_M	RT_V	FL_V	RT_L	FL_L	RT_P	FL_P	I&ET	MT(B)	MT(D)
7.66	0.000306	0.27	0.19	0.23	0.07	0.04	0.01	0.03	0.01	0.02	0.08	0.04	0.09	0.06
7.18	0.000655	0.19	0.09	0.27	0.04	0.05	0.01	0.04	0.00	0.00	0.04	0.04	0.10	0.07
7.66	0.000309	0.28	0.19	0.23	0.07	0.04	0.01	0.03	0.01	0.01	0.08	0.04	0.09	0.06
6.69	0.001375	0.08	0.04	0.33	0.03	0.06	0.00	0.04	0.00	0.01	0.02	0.04	0.10	0.08
7.18	0.000642	0.18	0.09	0.27	0.04	0.05	0.01	0.04	0.00	0.00	0.04	0.04	0.10	0.07
7.66	0.000300	0.27	0.19	0.23	0.07	0.04	0.01	0.03	0.01	0.01	0.08	0.04	0.10	0.06
7.66	0.000299	0.27	0.19	0.23	0.07	0.04	0.01	0.03	0.01	0.01	0.08	0.04	0.10	0.06

Seismic resilience values were calculated for the earthquakes shown in Table 4 considering several approaches: (a) a simple approach with no delay times and without non-structural elements (simple resilience), (b) an approach considering delay times with a bidding process (resilience W/DT-bidding), (c) an approach considering delay times with direct assignment (resilience W/DT-direct), (d) an approach considering both non-structural elements and delay times with the bidding process (resilience W/DT + NSE-bidding), and (e) an approach considering both non-structural elements and delay times with direct assignment (resilience w/DT + NSE -direct). The results are shown in Figure 23, where it is observed that there is a significant difference between resilience values for the different approaches presented. When using the simple approach, the resilience values are the highest, ranging from 95 to 100%. Incorporation of the delay times yielded resiliencies between 90 and 97%. Finally, the most refined approach considering delay times and non-structural elements produced resilience values of 82 to 96%, a variation of up to 13% when compared to the simple approach.

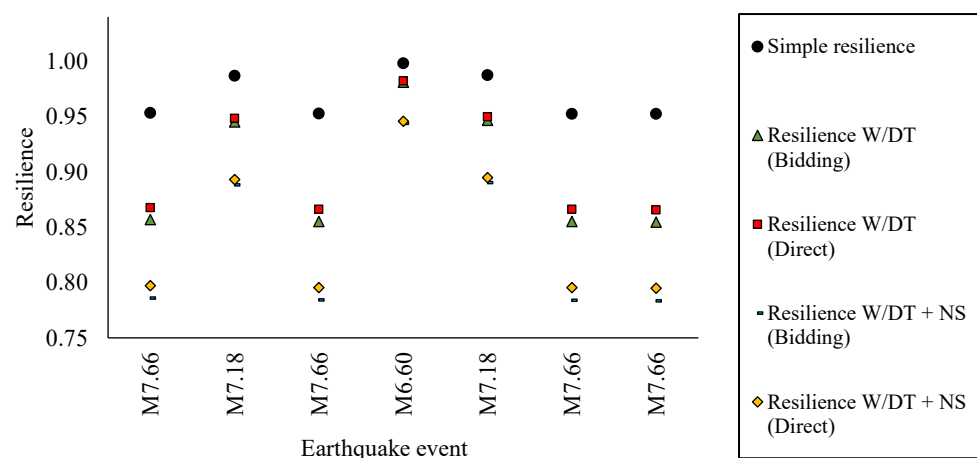


Figure 23. Estimated resilience for different events using several approaches.

As mentioned before, the delay time due to mobilization may be shortened by considering direct assignation, which may be accomplished by institutions in charge of planning for natural disasters. Figure 23 shows that resilience values can be increased by up to 3% (bidding vs. direct) by this action, which may be enough to upgrade a medium-resilience structure to a high-resilience one. This suggests that focusing on reducing delay times is a good method to improve the resilience of school infrastructure.

4.2. Acceptable Resilience Values

The resilience values previously obtained provide an estimation of the average functionality of a structure under a certain downtime given a seismic event; nonetheless, in order to use this information for decision making, it is still necessary to determine if such values are acceptable or not. In this research, a resilience-based classification is provided based on a cost–benefit (C/B) analysis, using Equation (7), where the minimum acceptable resilience value was estimated.

$$C/B = \frac{C_0 - L}{C_0} \quad (7)$$

In the previous equation, C_0 is the initial construction cost and L represents the losses produced from the downtime and repair activities. Since these losses depend on the amount of damage, they can be related to a parameter of structural response that represents this damage (for this particular case, the ductility demand is used); hence, the cost–benefit factor C/B can also be related to the structural response. For the group of structures under study, a given value of μ represents a certain damage, a certain recovery time, and a certain economic loss. Values of C/B as a function of μ are shown in Figure 24, showing that for values of μ approximately lower than 2, the C/B factor is positive, while

greater values of μ yield a negative cost/benefit. The shift between positive and negative C/B can be interpreted as its lowest acceptable value ($C/B = 0$) since it means that a structure can withstand the consequences of a strong ground motion without incurring losses greater than the initial construction cost. Furthermore, a $C/B = 0$ is associated with $\mu = 2$, which in turn is related to a repair time of 35%, meaning that the presented structures should exhibit repair times no greater than 35% of the maximum repair time possible to remain economically viable. On the other hand, according to the functionality loss model, a value of $\mu = 2$ is related to a functionality of 88%, which represents the minimum acceptable level of functionality a structure should maintain in a post-earthquake scenario. If Equation (1) is applied, considering a downtime of 35% with a functionality loss of 12% and considering the non-structural elements, then minimum acceptable resilience can be estimated as being equal to 92%. Such a value represents the lower resilience limit from an economic perspective and is highly relevant in resilience study since it could have important applications. For example, resilience values as low as 77% in school buildings have been reported in previous studies [43], which now can be categorized as structures with low resilience. Additionally, it is important to notice that, while these values are applicable to the structures in this study, the methodology can be used to define further acceptable values for other types of buildings.

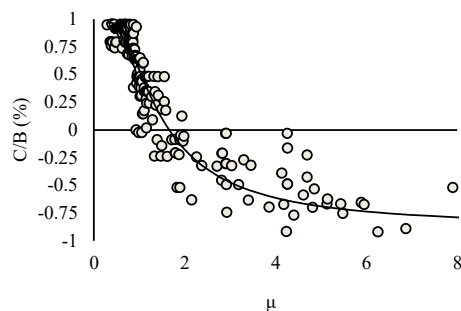


Figure 24. Cost–benefit vs. ductility demand and functionality loss vs. ductility demand.

Figure 24 shows that C/B is at a maximum (96%) up to a value of $\mu = 0.8$, which is associated with a repair time and functionality loss of 3.0% and 2.5%, respectively. When non-structural elements are taken into consideration and Equation (1) is used to calculate resilience, a value of 99% is obtained, which can be used to set a desirable resilience level indicative of structures capable of withstanding strong ground motion and maintaining high functionality with limited post-earthquake downtime, which in turn will directly address current social demands for the immediate re-occupancy of buildings after a natural disaster. Table 5 shows the proposal of a classification of resilience and resilience parameters in accordance with the previous discussions. This is a reference framework in resilience quantification and decision making due to the resilience values found, since researchers had previously only found resilience values [4,7] but not given a meaning to such quantities, at least from an analytical perspective.

Table 5. Resilience, functionality, and downtime classification for school buildings in Mexico.

Class	Resilience (R)	Time (RT)	Functionality (F)
High	$R \geq 99\%$	$RT \leq 3\%$	$F \geq 97.5\%$
Medium	$99\% > R > 92\%$	$3\% < RT < 35\%$	$97.5\% > F > 88\%$
Low	$R \leq 92\%$	$RT \geq 35\%$	$F \leq 88\%$

The previously proposed classification (Table 5) may be used to categorize quantified resilience for the seven critical seismic events, as shown in Figure 25 where the horizontal lines represent the high and low resilience limits. Evidently, the simplified approach regarding resilience quantification (simple resilience) leads to higher values near the upper

limit, and such values diminish along with the refinement of the resilience approach. When considering the delay times (resilience W/DT), the maximum resilience values decrease under the upper limit and the minimum values go under the lower limit. Finally, when the non-structural part is also added (resilience W/DT + NS), only one scenario (M6.6) demonstrates seismic resilience in the middle range, with all of the other events associated with a low resilience value. Another important aspect is the impact of the delay times in the resilience values, since, as shown in Figure 25, seismic resilience increases by up to 3% when taking into account a direct assignation process vs. a bidding process, which is significant since it is 40% of the increase required to upgrade from low to high resilience. This suggests that managing the delay times can be a crucial point to mitigating resilience loss. The previous discussions highlight the importance of continuing to refine the current approaches for resilience quantification, since simplifications can lead to important overestimations of actual resilience and, in the worst-case scenario, to underprepared communities.

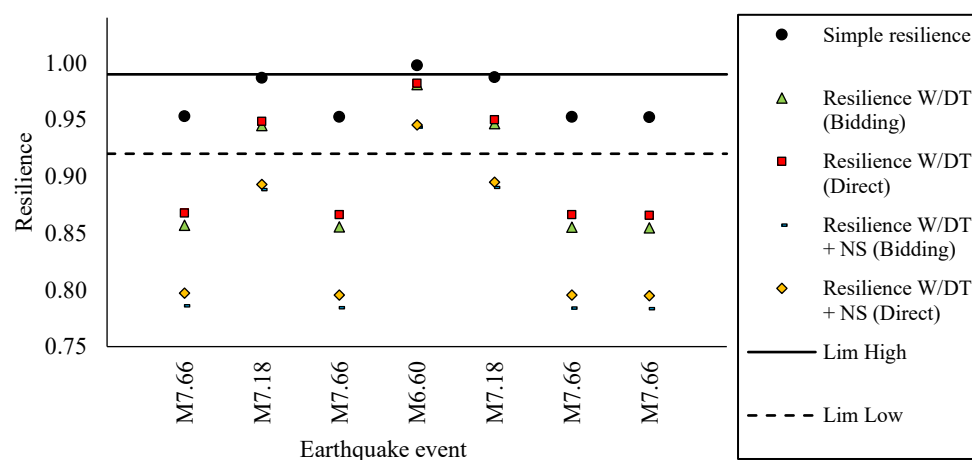


Figure 25. Estimated resilience for different events using several approaches and the acceptable resilience limits proposed.

Finally, recovery times (Figure 26), functionality (Figure 27), and seismic resilience (Figure 28) were quantified for all of the structures in the database using a refined approach (considering delay times and non-structural elements) to observe the distribution of these parameters in real community infrastructure in the state of Puebla given the occurrence of strong ground motion. Each of the aforementioned resilience parameters were analyzed under three intraplate seismic events: (a) an M6.69 earthquake, (b) an M7.18 earthquake, and (c) an M7.66 event.

During analysis of the recovery times (Figure 26), it was found that given the occurrence of seismic event A, the consequence in terms of RT would be an average RT of 1.5% (desirable range according to Table 5), with the main affected areas being in the southwest of the state of Puebla. Next, if seismic event B occurs, the consequence would be an average RT of 4.5%, with the main affected areas being in the south and center of the state, which means that a large amount of the structures would experience recovery times in the mid-range. On the other hand, the occurrence of seismic event C would provide a medium value of 9.5%, which is also in the intermediate RT range; however, maximum RT would reach up to 64%, significantly higher than the maximum acceptable limit (RT = 35%).

Analysis in terms of functionality loss (Figure 27) yields similar results to those of the RT analysis (Figure 26), presenting mean functionality loss values of 0.55%, 1.8%, and 4.8% for seismic events A, B, and C, achieving FL values higher than the admissible limit proposed in Table 5 in scenario C. This is reflected in the expected functionality maps shown in Figure 27.

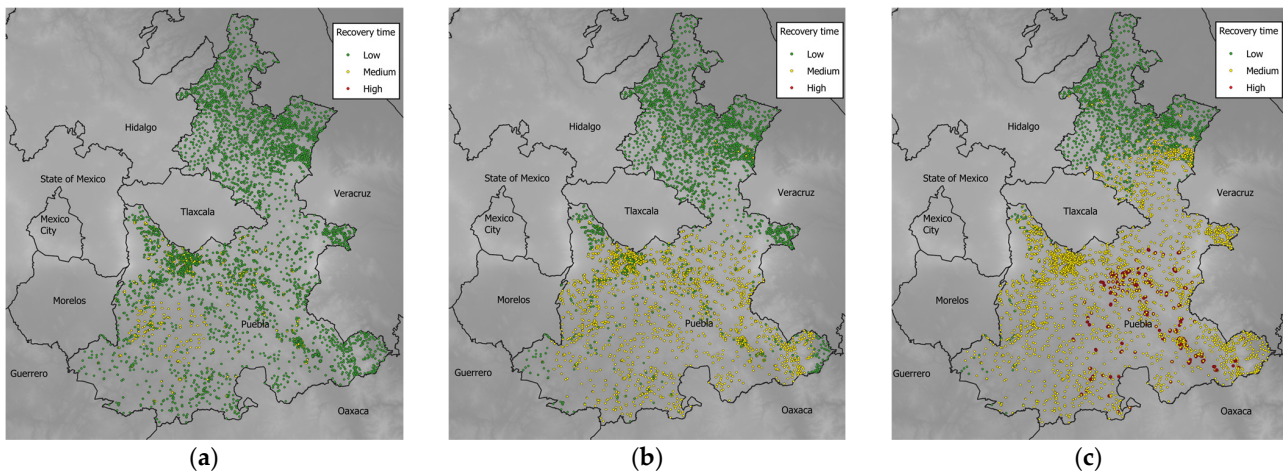


Figure 26. Expected recovery time maps for school buildings in Puebla after being subjected to strong ground motion: (a) M6.69; (b) M7.18; (c) M7.66.

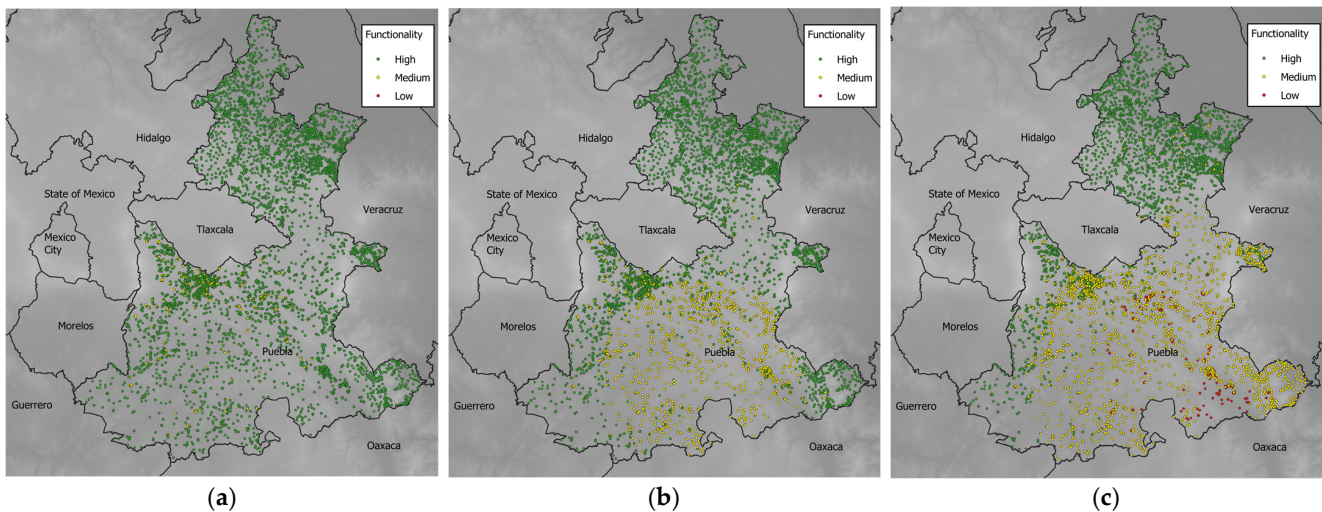


Figure 27. Expected functionality maps for school buildings in Puebla after being subjected to strong ground motion: (a) M6.69; (b) M7.18; (c) M7.66.

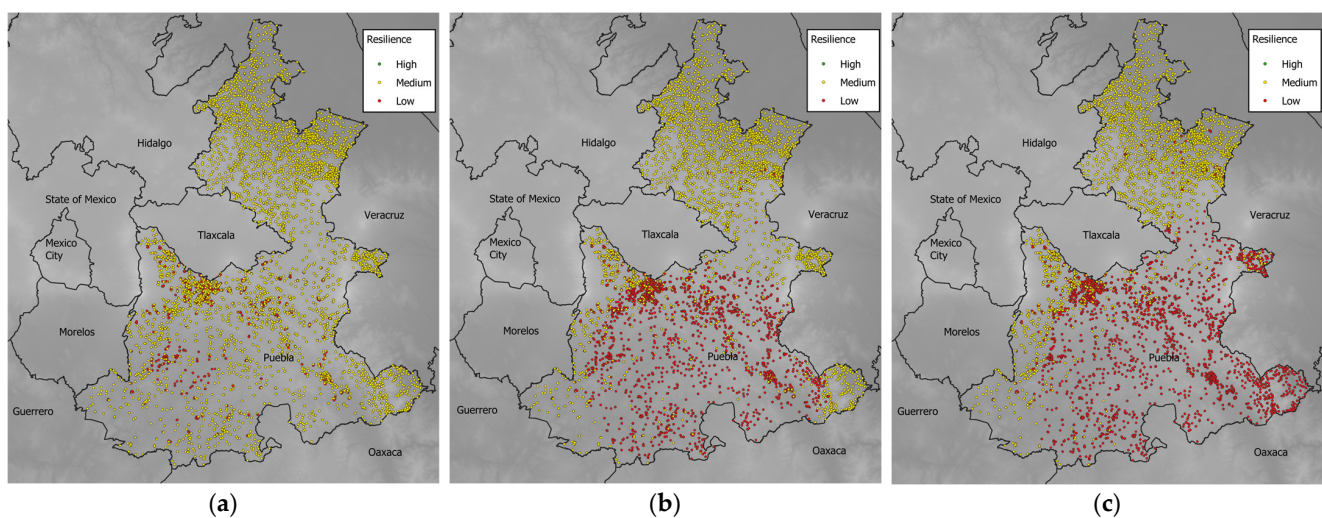


Figure 28. Expected resilience maps for school buildings in Puebla after being subjected to strong ground motion: (a) M6.69; (b) M7.18; (c) M7.66.

Finally, when resilience analysis including the effects of delay time and the affected non-structural components was performed, it was found that a hypothetical strong ground motion with the characteristics of scenario A would have a major effect on 9.5% of the structures, demonstrating low resilience values. Furthermore, the number of structures with low resilience increases to 38.7% given the occurrence of earthquake scenario B. Lastly, the intraplate M7.66 earthquake with normal faults associated with scenario C could have great negative consequences since 47.2% of the structures in the database exhibited resilience values under the minimum acceptable level, which may potentially lead to thousands of students without adequate facilities for a prolonged period of time and, in the worst scenario, result in various injuries and, probably, loss of human life. In addition, it is notable that in all three scenarios there is practically no presence of high resilience structures (under 1% of structures presented high values), which in this case is largely attributed to the delay times during the beginning of the recovery process, reinforcing the idea that resilience can be enhanced through control of the factors that delay the rehabilitation process.

5. Conclusions

This study focuses on providing a methodology to estimate resilience, through expected values functions for times and functionality, while taking into consideration delay times and non-structural elements. A comparison was carried out between simplified approaches for seismic estimation and refined ones. The results showed that a simplified approach to estimating seismic resilience is not reliable for decision making since it can lead to important overestimations of seismic resilience, and a more refined approach provides lower and thus more conservative values of resilience while maintaining a similar computational cost.

It was found that the study of delay time factors is highly relevant to resilience assessment since the shortening of some of these factors might increase seismic resilience, as in the case of direct assignation of structural repairing contracts instead of bidding processes.

There are few available studies regarding the definition of rating values for resilience; however, the method presented here suggests that cost–benefit analysis may be a good tool when defining acceptable resilience or downtime values from a financial point of view. For school buildings, a minimum acceptable value (mid-resilience limit) of 92% and a high resilience desirable value of 99% was found. When these acceptable and desired values were compared to resilience values reported in previous research (González et al., 2018), it was found that the analyzed structure presented low resilience in most cases.

From the resilience analysis presented on school buildings in Puebla city, it is evident that prevention measures must be taken alongside the development of post-earthquake contingency plans in order to increase educative infrastructure resilience since strong ground motion earthquakes could have major impacts on the education sector with its current conditions.

Author Contributions: Conceptualization, C.G. and M.N.; methodology, C.G. and M.N.; software, C.G.; validation, M.N. and G.A.; formal analysis, C.G. and M.N.; investigation, C.G. and M.N.; resources, C.G. and M.N.; data curation, M.N. and G.A.; writing—original draft preparation, C.G. and M.N.; writing—review and editing, M.N. and G.A.; visualization, M.N. and G.A.; supervision, M.N. and G.A.; project administration, M.N.; funding acquisition, M.N. All authors have read and agreed to the published version of the manuscript.

Funding: This research was funded by the National Council of Science and Technology (CONACyT), Project number A1-S-35223, “Seismic demands definition for the risk and resilience-based design of structures”.

Acknowledgments: The first author thanks the National Council of Science and Technology (CONACyT) for the Ph.D. scholarship awarded.

Conflicts of Interest: The authors declare no conflict of interest. The funders had no role in the design of the study; in the collection, analyses, or interpretation of data; in the writing of the manuscript; or in the decision to publish the results.

References

1. Ortiz, D.; Reinoso, E. Tiempo de interrupción de negocios en la ciudad de México por daños directos y efectos indirectos en edificios a causa del sismo del 19s de 2017. *Rev. De Ing. Sísmica* **2020**, *104*, 1–31. (In Spanish) [CrossRef]
2. Bruneau, M.; Chang, S.; Eguchi, R.; Lee, G.; O'Rourke, T.; Reinhorn, A.; Winterfeldt, D. A framework to quantitatively assess and enhance the seismic resilience of communities. *Earthq. Spectra* **2003**, *19*, 733–752. [CrossRef]
3. Bruneau, M.; Reinhorn, A. Exploring the concept of seismic resilience for acute care facilities. *Earthq. Spectra* **2007**, *23*, 41–62. [CrossRef]
4. Cimellaro, G.; Reinhorn, A.; Bruneau, M. Framework for analytical quantification of disaster resilience. *Eng. Struct.* **2010**, *32*, 3639–3649. [CrossRef]
5. Anwar, G.; Dong, Y.; Zhai, C. Performance-based probabilistic framework for seismic risk, resilience, and sustainability assessment of reinforced concrete structures. *Adv. Struct. Eng.* **2019**, *23*, 1454–1472. [CrossRef]
6. Biondini, F.; Cannasio, E.; Titi, A. Seismic resilience of concrete structures under corrosion. *Earthq. Eng. Struct. Dyn.* **2015**, *44*, 2445–2466. [CrossRef]
7. González, C.; Niño, M.; Jaimes, M. Event-based assessment of seismic resilience in Mexican school buildings. *Bull. Earthq. Eng.* **2020**, *18*, 6313–6336. [CrossRef]
8. Rojahn, C.; Johnson, L.; O'Rourke, T.; Cedillos, V.; McAllister, T.; McCabe, S. Increasing Community Resilience Through Improved Lifeline Infrastructure Performance. *Bridge*. 2019. Available online: <https://www.nae.edu/212179/Increasing-Community-Resilience-through-Improved-Lifeline-Infrastructure-Performance> (accessed on 28 January 2023).
9. Feng, K.; Wang, N.; Li, Q.; Lin, P. Measuring and enhancing resilience of building portfolios considering the functional interdependence among community sectors. *Struct. Saf.* **2017**, *66*, 118–126. [CrossRef]
10. Fontana, C.; Cianci, E.; Moscatelli, M. Assessing Seismic Resilience of School Educational Sector. An attempt to establish the initial conditions in Calabria Region, Southern Italy. *Int. J. Disaster Risk Reduct.* **2020**, *51*, 101936. [CrossRef]
11. Ruggieri, S.; Perrone, D.; Leone, M.; Uva, G.; Aiello, M.A. A prioritization RVS methodology for the seismic risk assessment of RC school buildings. *Int. J. Disaster Risk Reduct.* **2020**, *51*, 101807. [CrossRef]
12. Ruggieri, S.; Porco, F.; Uva, G.; Vamvatsikos, D. Two frugal options to assess class fragility and seismic safety for low-rise reinforced concrete school buildings in Southern Italy. *Bull. Earthq. Eng.* **2021**, *19*, 1415–1439. [CrossRef]
13. Samadian, D.; Ghafoy-Ashtiany, M.; Naderpour, H.; Eghbali, M. Seismic resilience evaluation based on vulnerability curves for existing and retrofitted typical RC school buildings. *Soil Dyn. Earthq. Eng.* **2019**, *127*, 105844. [CrossRef]
14. Gutiérrez, J.; Ayala, G. Análisis de la resiliencia sísmica de edificios. *Ing. Sísmica* **2022**, *107*, 47–73. [CrossRef]
15. Almufti, I.; Willford, M. *Resilience-based Earthquake Design Initiative for the Next Generation of Buildings*; Arup: San Francisco, CA, USA, 2013. [CrossRef]
16. Mieler, M.; Stojadinovic, B.; Budnitz, R.; Comerio, M.; Mahin, S. A framework for linking community-resilience goals to specific performance targets for the built environment. *Earthq. Spectra* **2015**, *31*, 1267–1283. [CrossRef]
17. Hall, D.; Giglio, N. *Architectural Graphic Standards*, 12th ed.; American Institute of Architects: Washington, DC, USA, 2016.
18. Yang, T.Y.; Tung, D.P.; Li, Y. Equivalent Energy Design Procedure for Earthquake Resilient Fused Structures. *Earthq. Spectra* **2018**, *34*, 795–815. [CrossRef]
19. Tena-Colunga, A.; Nangullasmú-Hernández, H. Resilient seismic design of reinforced concrete framed buildings with metallic fuses including soil-structure interaction effects. *Soil Dyn. Earthq. Eng.* **2023**, *164*, 137. [CrossRef]
20. Ibarra, L.F.; Medina, R.A.; Krawinkler, H. Hysteretic models that incorporate strength and stiffness deterioration. *Earthq. Engng. Struct. Dyn.* **2005**, *34*, 1489–1511. [CrossRef]
21. Tsionis, G. *Seismic Resilience: Concept, Metrics and Integration with Other Hazards*; Joint Research Center: Luxembourg, 2014.
22. Taghavi, S.; Miranda, E. *Response Assessment of Nonstructural Building Elements*, 1st ed.; Pacific Earthquake Engineering Research Center: Berkeley, CA, USA, 2003; pp. 57–66.
23. Ghorawat, S. Rapid Loss Modeling of Death and Downtime Caused by Earthquake Induced Damage to Structures. Master's Thesis, Texas A&M University, College Station, TX, USA, May 2011.
24. Comerio, M.C. Estimating Downtime in Loss Modeling. *Earthq. Spectra* **2006**, *22*, 349–365. [CrossRef]
25. Alcocer, S.; Bautista, R.; Martínez, Y.; Valencia, G. Desarrollo de capacidades nacionales para aumentar la resiliencia de edificios de concreto y mampostería con un enfoque de diseño por desempeño. In *Revisión de la Literatura y del Estado del Arte de Metodologías de Evaluación Post-Sísmica*, 1st ed.; Instituto de Ingeniería UNAM: Ciudad de México, México, 2019; pp. 3–58.
26. Alcocer, S.; Muria, D.; Abarca, J.; Bautista, R.; Bogoya, G.; Cruz, V.; Martínez, Y.; Moctezuma, B.; Ramírez, D.; Valencia, G. *Guía técnica para la Rehabilitación Sísmica de Edificios Escolares de la Ciudad de México*, 1st ed.; Instituto de Ingeniería UNAM: Ciudad de México, México, 2019; pp. 55–169.
27. Alcocer, S.; Muria, D.; Fernández, L.; Ordaz, M.; Arce, J. Observed damage in public school buildings during the 2017 Mexico earthquakes. *Earthq. Spectra* **2020**, *36*, 110–129. [CrossRef]
28. McKenna, F.; Mazzooni, S.; Scott, M.; Fenves, G. *Open System for Earthquake Engineering Simulation Version 3.2.0.*; Pacific Earthquake Engineering Research Center: Berkeley, CA, USA, 2016.
29. Newmark, N.M.; Hall, W.J. *Seismic Design Criteria for Nuclear Reactor Facilities*. Rep. No. 46; Building Practices for Disaster Mitigation National Bureau of Standards: Washington, DC, USA, 1973; pp. 209–236.

30. Hidalgo, P.A.; Arias, A. New Chilean code for earthquake resistant design of buildings. In Proceedings of the 4th US National Conference on Earthquake Engineering, Palm Springs, CA, USA, 20–24 May 1990; Volume 2, pp. 927–936.
31. Tanik, B.; Inel, M.; Ozer, E. Effect of Soil-Structure interaction on seismic behavior of mid- and low-rise buildings. *ASCE Int. J. Geomech.* **2021**, *21*, 04021009. [[CrossRef](#)]
32. Vamvatsikos, D.; Cornell, A. Incremental Dynamic Analysis. *Earthq. Eng. Struct. Dyn.* **2002**, *31*, 491–514. [[CrossRef](#)]
33. Forte, A.; Santini, S.; Lavorato, D.; Fiorentino, G. Influence of material knowledge on the assessment of shear strength characteristic value on existing RC beams. In Proceedings of the 12th fib International PhD Symposium in Civil Engineering, Prague, Czech Republic, 29–31 August 2018.
34. Gobierno Ciudad de México. *Normas para la Rehabilitación Sísmica de Edificios de Concreto Dañados por el Sismo del 19 de Septiembre de 2017*; Gaceta Oficial de la Ciudad de México: Ciudad de México, México, 2017; pp. 6–17.
35. FEMA-P-58. *Seismic Performance Assessment of Buildings, 1 Methodology*, 2nd ed.; Federal Emergency Management Agency: Redwood City, CA, USA, 2018; pp. 3.1–3.38.
36. Baggio, C.; Bernardini, A.; Colozza, R.; Corazza, L.; Della Bella, M.; Di Paaquele, G.; Dolce, M.; Orsini, G.; Papa, F.; Zuccaro, G. *Field Manual for Post-Earthquake Damage and Safety Assessment and Short-Term Countermeasures*; EUR 22868 EN. JRC37914; Office for Official Publications of the European Communities: Luxembourg, 2007.
37. INIFED. *Estrategias y Mecanismos de Coordinación para la Evaluación y Validación de Daños*; SEP-INIFED: Ciudad de México, México, 2017.
38. Noyola, V.; Soca, J.; Aguilera, M.; Martínez, O. *Infraestructura, Mobiliario y Materiales de Apoyo Educativo en las Escuelas Primarias ECEA 2014*, 1st ed.; INEE: Ciudad de México, México, 2016; pp. 21–82.
39. FEMA-P-58-2. *Seismic Performance Assessment of Buildings, 2 Implementation Guide*, 2nd ed.; Federal Emergency Management Agency: Redwood City, CA, USA, 2018; pp. 2.11–2.15.
40. Jaimes, M.; Candia, G. Seismic risk of sliding ground-mounted rigid equipment. *Eng. Struct.* **2020**, *204*, 110066. [[CrossRef](#)]
41. Jaimes, M.; Niño, M. Cost-Benefit analysis to assess seismic mitigation options in Mexican public-school buildings. *Bull. Earthq. Eng.* **2017**, *15*, 3919–3942. [[CrossRef](#)]
42. Cardona, O.; Ordaz, M.; Reinoso, E.; Yamín, L.B.; Barbat, A.H. CAPRA- Comprehensive approach to probabilistic risk assessment: International initiative for risk management effectiveness. In Proceedings of the 15th World Conference on Earthquake Engineering, Lisbon, Portugal, 24–28 September 2012.
43. González, C.; Niño, M.; Jaimes, M. Seismic resilience estimation in public school buildings. In Proceedings of the XXI National Congress on Structural Engineering, Campeche, México, 19–21 May 2018.

Disclaimer/Publisher’s Note: The statements, opinions and data contained in all publications are solely those of the individual author(s) and contributor(s) and not of MDPI and/or the editor(s). MDPI and/or the editor(s) disclaim responsibility for any injury to people or property resulting from any ideas, methods, instructions or products referred to in the content.